

ARMY RESEARCH LABORATORY



# Simulating Sympathetic Detonation of 105-mm Artillery Projectiles with CTH

by Kelly J. Benjamin  
and John Starkenberg

ARL-TR-1365

June 1997

DTIC QUALITY INSPECTED \*

19970623 074

Approved for public release; distribution is unlimited.

The findings in this report are not to be construed as an official Department of the Army position unless so designated by other authorized documents.

Citation of manufacturer's or trade names does not constitute an official endorsement or approval of the use thereof.

Destroy this report when it is no longer need. Do not return it to the originator.

# **Army Research Laboratory**

Aberdeen Proving Ground, MD 21005-5066

---

---

**ARL-TR-1365**

**June 1997**

---

## **Simulating Sympathetic Detonation of 105-mm Artillery Projectiles with CTH**

**Kelly J. Benjamin, John Starkenberg**  
Weapons and Materials Research Directorate, ARL

---

## Abstract

---

The CTH code was used to simulate sympathetic detonation experiments conducted using 105-mm projectiles separated by buffers of Plexiglas, rolled homogeneous armor (RHA), and mild steel. Buffer thicknesses near the experimental sympathetic detonation threshold were simulated. No propagation criterion associated with pressure loading was revealed by the results of this study. CTH computations were also made to confirm the presence of finite rise-time or "ramp" waves in the acceptor explosive (previously observed in Lagrangian computations) with layered buffers of Plexiglas and steel. The CTH results show more structure in the ramp wave and shorter rise times than those previously obtained. The History Variable Reactive Burn (HVRB) explosive initiation model in the CTH code was exercised in simulations of similar configurations. These simulations showed that initiation may occur during propagation of the incident shock wave through the acceptor or after its reflection from the casing at the back of the acceptor. Predicted buffer thicknesses required to prevent sympathetic detonation are much less than those determined in the experiments, indicating that mechanisms in addition to shock initiation contribute to sympathetic detonation.

## TABLE OF CONTENTS

		<u>Page</u>
	LIST OF FIGURES .....	v
	LIST OF TABLES .....	vii
1.	INTRODUCTION .....	1
2.	DESCRIPTION OF CTH .....	1
3.	BRIEF DESCRIPTION OF THE EXPERIMENTS .....	2
4.	CTH SIMULATION OF THE EXPERIMENTS .....	2
5.	COMPARISON OF CTH AND STEALTH COMPUTATIONS .....	4
6.	HVRB PREDICTIONS OF SYMPATHETIC DETONATION .....	5
7.	SUMMARY AND CONCLUSIONS .....	5
8.	REFERENCES .....	27
	DISTRIBUTION LIST .....	29
	REPORT DOCUMENTATION PAGE .....	33

INTENTIONALLY LEFT BLANK.

## LIST OF FIGURES

<u>Figure</u>	<u>Page</u>
1. Experimental arrangement used by Boyle .....	7
2. 2-D CTH simulation .....	9
3. 76-mm Plexiglas buffer: contour plot sequence .....	10
4. 76-mm Plexiglas buffer: pressure history .....	11
5. 76-mm Plexiglas buffer: impulse history .....	12
6. Plexiglas and mild steel: comparison of pressure contours .....	13
7. Plexiglas and mild steel: comparison of pressure and impulse histories .....	14
8. Mild steel and RHA: comparison of pressure contours at the experimental threshold .....	15
9. Mild steel and RHA: comparison of pressure and impulse histories at the experimental threshold .....	16
10. Mild steel and RHA: comparison of pressure contours at the same buffer thickness .....	17
11. Mild steel and RHA: comparison of pressure and impulse histories at the same buffer thickness .....	18
12. Results of the STEALTH sympathetic detonation simulation with layered buffers .	20
13. Results of the CTH sympathetic detonation simulation with layered buffers .....	21
14. Unbuffered configuration with 12.7-mm separation: pressure and reaction variable contours .....	22
15. 6.4-mm Steel buffer in direct contact with donor and acceptor munitions: pressure and reaction variable contours .....	23
16. 6.4-mm Plexiglas buffer centered in 12.7-mm space: pressure and reaction variable contours .....	24

INTENTIONALLY LEFT BLANK.



## LIST OF TABLES

<u>Table</u>	<u>Page</u>
1. Experimental Results .....	8
2. Computed Pressure and Impulse at the Experimental Thresholds .....	19
3. Sympathetic Detonation Predictions for the Contact Configuration .....	25
4. HVRB Results for 12.7-mm Munition-to-Munition Separation Computations ...	26

INTENTIONALLY LEFT BLANK.

## 1. INTRODUCTION

Sympathetic detonation of munitions occurs when a detonating munition (the donor) initiates detonation in a neighboring munition (the acceptor). Shock due to casing impact is the primary propagation mechanism for unshielded munitions at close range, while at longer range, fragment penetration is the primary mechanism. Shielding (buffers) between munitions reduces the incidence of sympathetic detonation by reducing shock stimulus and impeding fragments.

The present study employed the CTH code (Hertel et al. 1993) and focused on three objectives. The first was to determine if any similarities in pressure-loading exist when using CTH to simulate buffered sympathetic detonation experiments with buffer thicknesses near the sympathetic detonation threshold, as determined in experiments. The second objective was to confirm the presence of finite rise-time or "ramp" waves in the acceptor explosive previously observed using the nonreactive Lagrangian code STEALTH (Electric Power Research Institute 1981). The third objective was to exercise a CTH reactive model within the acceptor explosive.

## 2. DESCRIPTION OF CTH

The continuum mechanics solver CTH is an ongoing project of the Sandia National Laboratory. It is intended to provide capabilities for modeling dynamics of multidimensional systems with multiple materials, large deformations and strong shock waves. Finite-difference analogs of the Lagrangian equations of momentum and energy conservation are employed with continuous rezoning to construct Eulerian differencing. Shock and detonation waves are treated using the method of artificial viscosity. CTH makes use of analytic (Mie-Gruneisen, JWL, etc.) and tabular (Sesame) equations of state as well as modern constitutive models (Johnson-Cook, Zerilli-Armstrong) including fracture (void insertion). In addition, there are three reaction models (Programmed Burn, CJ Volume Burn and History Variable Reactive Burn [HVRB]) and two porosity models. A variety of plots of computed results can be produced. These options provide an opportunity to treat complex material behavior including melting, vaporization, solid phase transitions, chemical reaction, and electronic excitation and ionization.

### 3. BRIEF DESCRIPTION OF THE EXPERIMENTS

The experimental arrangement (Boyle 1995) is illustrated in Figure 1. Both the donor and the acceptor munitions were 105-mm projectiles. In each experiment, the donor was filled with Composition B and the acceptor with pentolite. Each donor was initiated at a point on the side farthest from the acceptor, halfway between its top and bottom. Potted carbon gauges and steel witness plates were used to record the results. Buffer materials included polyethylene, mild steel, and rolled homogeneous armor (RHA). All buffers were 203 mm wide and 510 mm high. The thickness of the buffers was varied in order to determine a sympathetic detonation threshold.

The experimental results are summarized in Table 1. The "GOs" represent configurations in which sympathetic detonation of the acceptor occurred, while the "NOGOs" indicate that sympathetic detonation did not occur. Threshold ranges obtained from these results determined the buffer thicknesses we simulated computationally.

### 4. CTH SIMULATION OF THE EXPERIMENTS

The 2-D CTH simulation (representing the cross-sectional plane in which the donor is initiated) is illustrated in Figure 2. The primary effect of simulating a 3-D experiment in 2-D is to decrease the rate of decay of spherically divergent waves to that of cylindrically divergent waves. This produces somewhat higher stimulus levels in the 2-D case. The experiments were simulated with buffer thicknesses near the sympathetic detonation threshold for each buffer material. The dimensions were consistent with M1 105-mm projectiles. Casings were 10-mm-thick mild steel. The donor munition was filled with Composition B, modeled using a JWL equation of state for detonation products. The acceptor fill was "inert" pentolite, represented by a JWL equation of state with estimated constants. The donor munition was initiated at the side farthest from the acceptor using the programmed burn model. All buffers were 203 mm wide. Plexiglas was substituted for polyethylene, which was used as a buffer material in some of the original experiments. The buffer thicknesses were 70 mm and 76 mm for the Plexiglas buffers, 32 mm and

38 mm for the mild-steel buffers, and 38 mm and 51 mm for the RHA buffers. In addition to the threshold computations, a computation was made with a 38-mm-thick RHA buffer to enable direct comparison with the mild-steel computation at the same thickness.

Figure 3 shows a sequence of pressure contour plots for the Plexiglas buffer. The programmed burn detonation can be seen propagating across the donor munition in the first frame, while subsequent frames illustrate a shock wave propagating through the buffer and casing of the acceptor and into the acceptor explosive. The buffer is nearly obliterated and the acceptor is significantly deformed at late times. A crack can be seen in the casing at the back of the acceptor in the last frame. Figures 4 and 5 illustrate pressure and impulse history plots, respectively, from the same computation, taken at a point just inside the acceptor casing. The loading consists of an initial pulse about 40  $\mu$ s wide, followed by significant late-time reverberations. The impulse history plot indicates that about half the ultimate impulse delivered is associated with the reverberations.

Figure 6 is a comparison of pressure contour plots for the Plexiglas buffer with similar plots for a mild-steel buffer. The shock arrives at the acceptor explosive 15  $\mu$ s sooner in the mild-steel buffer simulation, due to the smaller thickness of and higher wave speed in the steel. Otherwise, the results from both the Plexiglas and mild-steel buffer simulations appear similar. At late times, some cracking on the front of the acceptor near the center can be observed with the steel buffer and acceptor casing, but no cracking is seen at the back of the casing. As illustrated in Figure 7, significant differences in pressure-loading are indicated in the pressure and impulse history plots. With the mild-steel buffer, the initial pulse is higher and narrower and the late-time pressures remain insignificant. Thus, though the impulse associated with the initial pulse is higher with the mild-steel buffer, the ultimate impulse is higher with the Plexiglas buffer.

Figure 8 illustrates a comparison of pressure contour plots for the 38-mm mild-steel buffer and the 51-mm RHA buffer. With the RHA buffer, a more definite cracking response can be seen in the acceptor casing on the side near the buffer, but otherwise the results appear similar. A

comparison of the pressure and impulse history plots of the RHA and mild-steel buffers, as shown in Figure 9, reveals no significant differences except that the pressures are somewhat higher and the ultimate impulse is significantly higher with the mild-steel buffer.

Figure 10 shows a comparison of pressure contour plots between a 38-mm RHA buffer and a 38-mm mild-steel buffer. With the buffer thicknesses equal, the RHA shows greater resistance to deformation and cracks clearly at late times. The pressure and impulse history plots are similar, as shown in Figure 11. The initial peak pressure is slightly higher and the ultimate impulse is somewhat lower with the RHA buffer.

The pressure and impulse results at the experimental threshold are summarized in Table 2. The impulse at the end of the first pulse, as well as the ultimate impulse (defined as the value at 250  $\mu$ s) is included. As shown in the table, the peak pressure is the same for Plexiglas and RHA, but higher for mild steel. The first-pulse impulse is different for all three buffer materials. The ultimate impulse values are similar for Plexiglas and mild steel, but lower for RHA.

## 5. COMPARISON OF CTH AND STEALTH COMPUTATIONS

CTH computations were performed to compare with the results obtained in a previous sympathetic detonation study, which used the nonreactive Lagrangian code STEALTH (Starkenberget al. 1987). In the STEALTH study, ramp waves as long as 25  $\mu$ s were observed in the acceptor explosive when layered buffers were used between munitions. In one case, the layered buffers consisted of 10 mm of Plexiglas sandwiched between two 10-mm layers of steel. Figures 12 and 13 show pressure waveforms produced in the acceptor munition in STEALTH and CTH simulations of the same configuration. The results obtained with CTH show more structure in the ramp wave and shorter rise-times than those obtained with STEALTH.

## 6. HVRB PREDICTIONS OF SYMPATHETIC DETONATION

The HVRB explosive initiation model (Kerley 1992) was exercised in two series of CTH simulations. In one series, the donor and acceptor were in direct contact with the buffer. In the other, the donor and acceptor were separated by a fixed 12.7-mm space, and the buffer was centered in that space. In both series, the acceptors were filled with reactive Composition B, and buffer thicknesses were decreased until sympathetic detonation occurred.

Figure 14 shows a sequence of pressure and reaction variable contour plots for unbuffered projectiles separated by a 12.7-mm space. Pressure contours are shown on the right side, and reaction variable contours are shown on the left side of each plot. In this case, initiation of the acceptor occurs as the incident shock wave propagates through it.

A sequence of contour plots for a 6.4-mm-thick steel buffer in direct contact with the donor and acceptor munitions is shown in Figure 15. This illustrates a configuration that does not produce sympathetic detonation.

Figure 16 shows a sequence of pressure and reaction variable contour plots for a 6.4-mm Plexiglas buffer centered in a 12.7-mm space. Initiation of the acceptor occurs after reflection of the shock wave at 55  $\mu$ s.

The results obtained in the HVRB simulations are summarized in Tables 3 and 4. In all cases, the buffer thicknesses required to prevent sympathetic detonation are less than those required in the experiments.

## 7. SUMMARY AND CONCLUSIONS

We simulated sympathetic detonation experiments with buffers at the threshold thickness. No propagation criterion associated with pressure-loading was revealed by the results of this study.

Buffers may prevent sympathetic detonation by influencing other aspects of the loading in addition to pressure. We observed that low-impedance Plexiglas buffers tend to spread out the pressure-loading over a longer period of time, while the high-strength steel and RHA buffers reduce deformation and damage.

When layered buffers are used, the results obtained with CTH show more structure in the ramp wave and shorter rise-times than those previously obtained with STEALTH. The response of explosives to ramp waves is not well understood, but it has been observed to be less violent than to a shock wave of the same strength.

Simulations with the HVRB explosive initiation model show that shock initiation may occur during propagation of the incident shock wave through the acceptor or after its reflection from the casing at the back of the acceptor. Buffers required to prevent sympathetic detonation in the computations were much thinner than those required in the experiments. This is another indication that mechanisms in addition to shock initiation contribute to sympathetic detonation. These results contrast sharply with those obtained in an earlier study using the Forest Fire initiation model and the 2DE code (Starkenbergh, Huang, and Arbuckle 1984). In that study, no buffer that could prevent sympathetic detonation of Composite B-filled 105-mm projectiles was found.



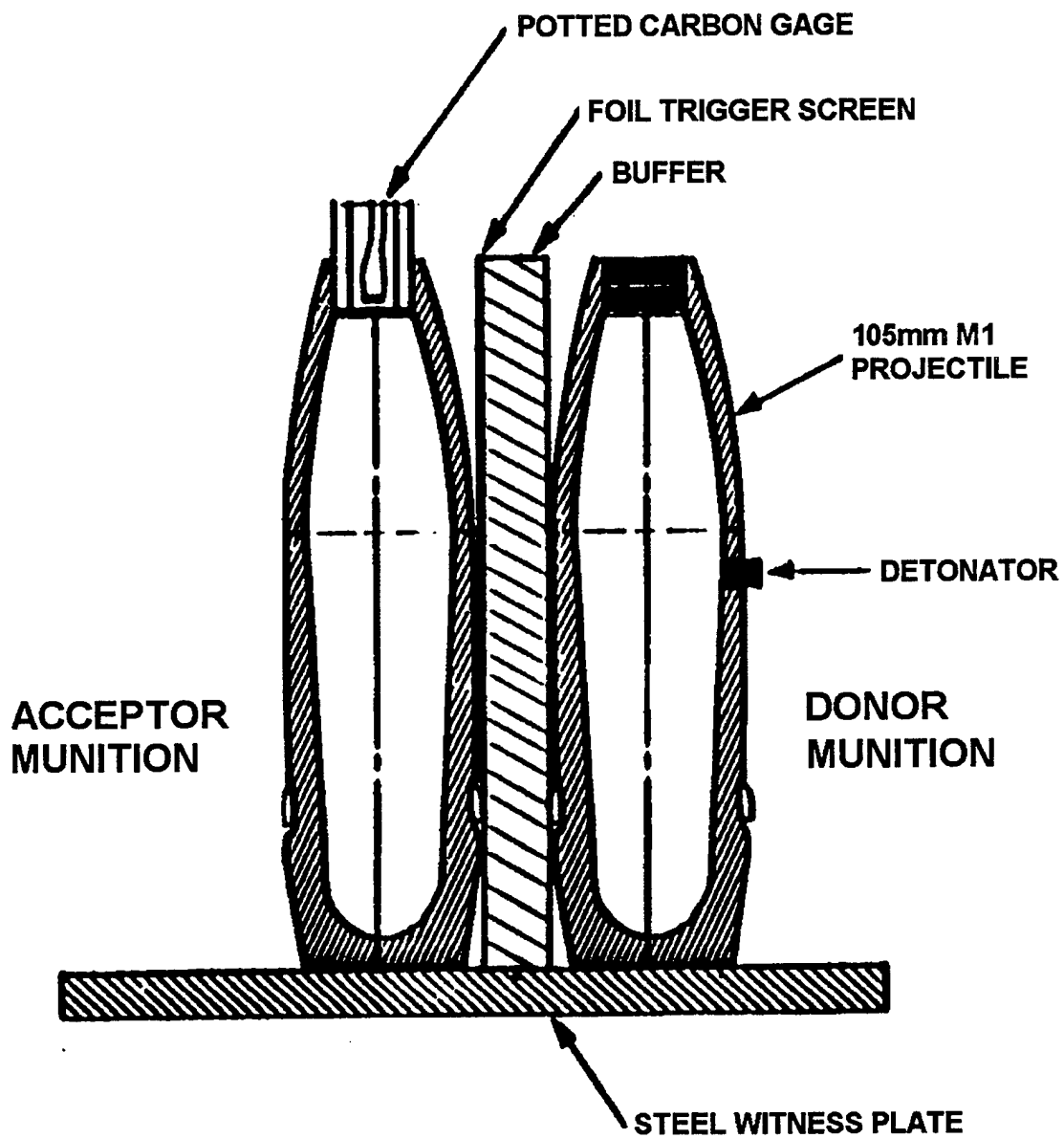


Figure 1. Experimental arrangement used by Boyle.

Table 1. Experimental Results

MATERIAL	THICKNESS (mm)	RESULT
MILD STEEL	<38	4 GOs
	38	NOGO
	38	NOGO
	>38	3 NOGOs
RHA	<51	2 GOs
	51	GO
	51	NOGO
	>51	3 NOGOs
POLYETHYLENE	<70	5 GOs
	70	GO
	70	NOGO
	76	GO
	76	NOGO
	76	NOGO
	>76	3 NOGOs

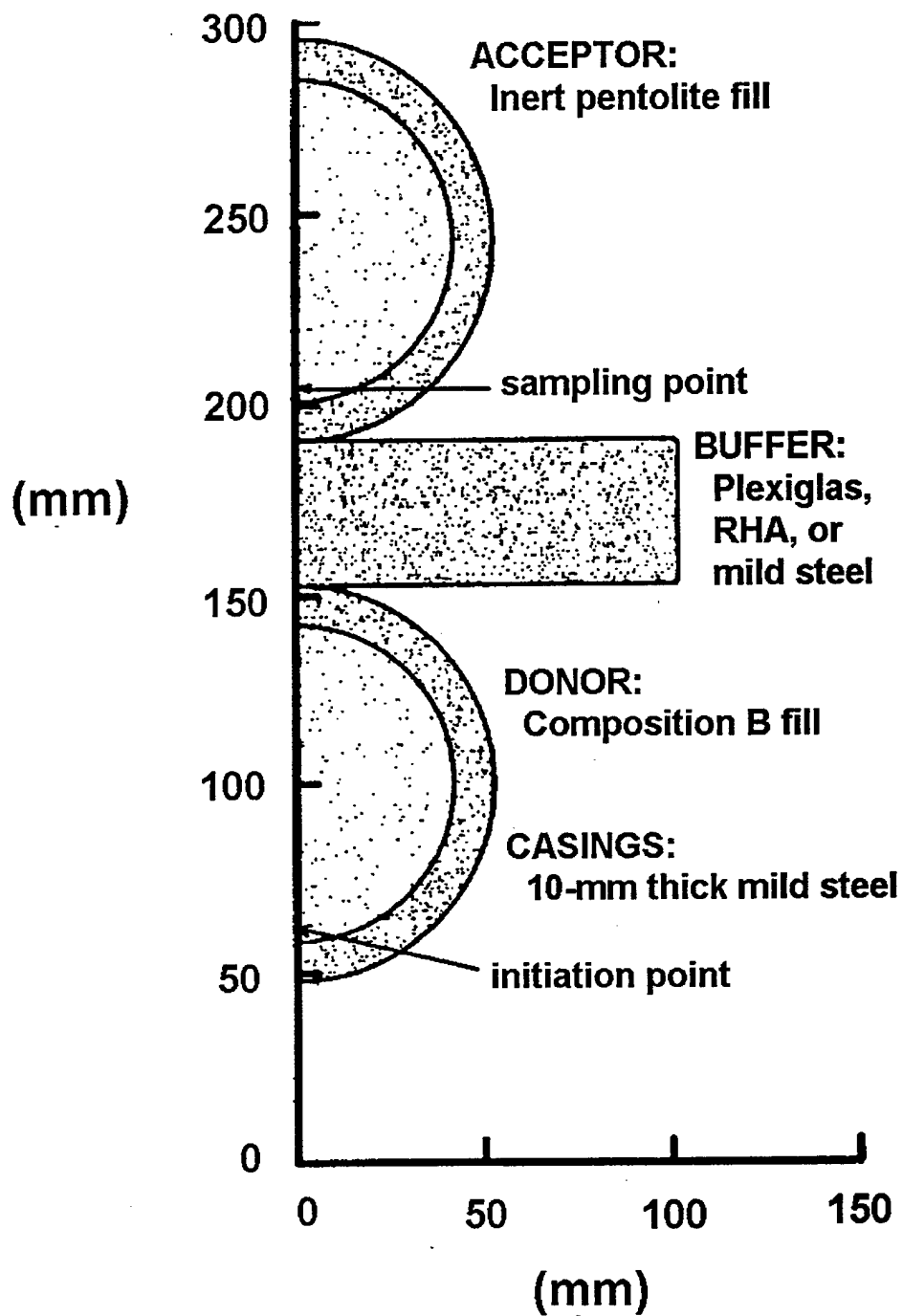


Figure 2. 2-D CTH Simulation.

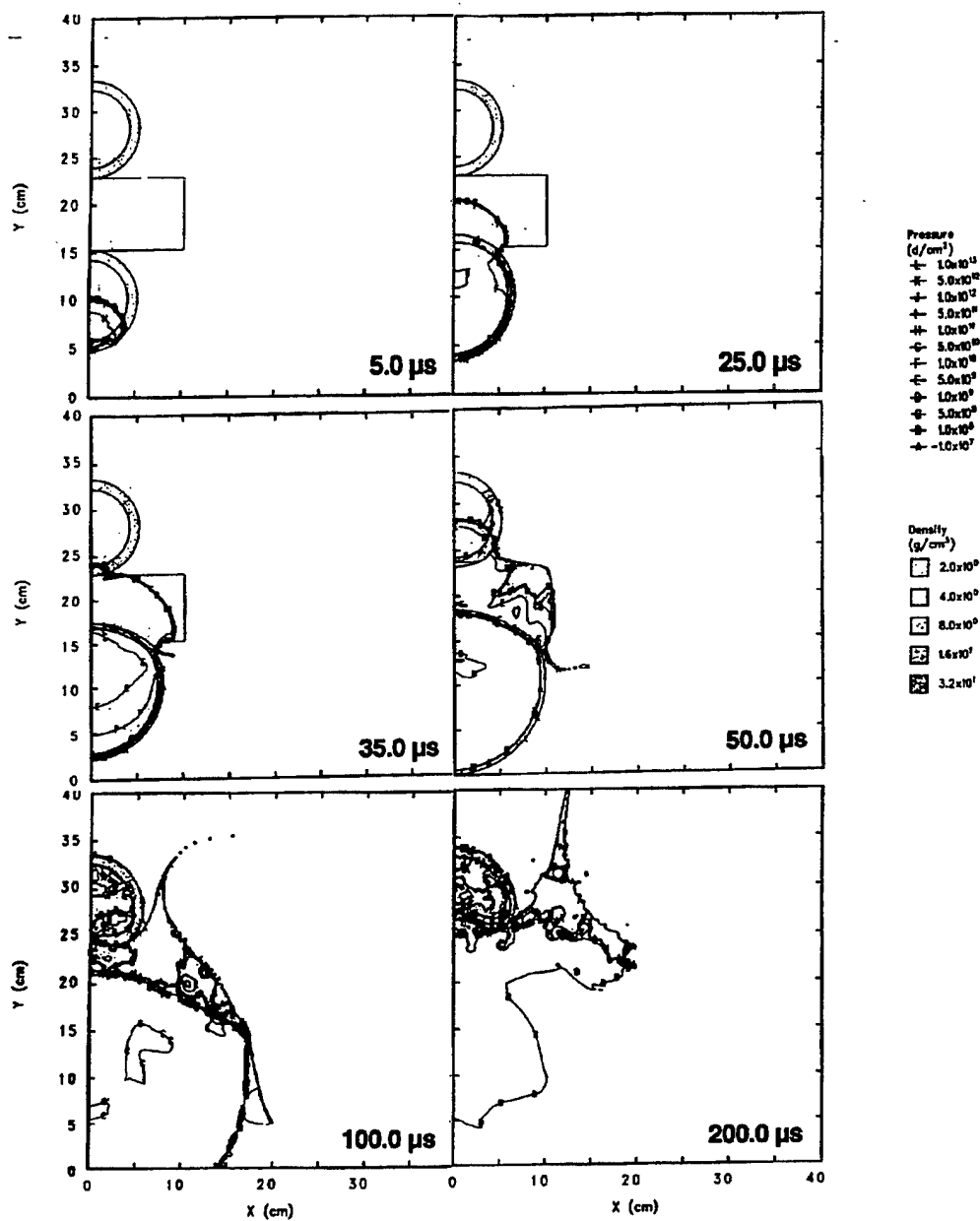


Figure 3. 76-mm Plexiglas buffer: contour plot sequence.

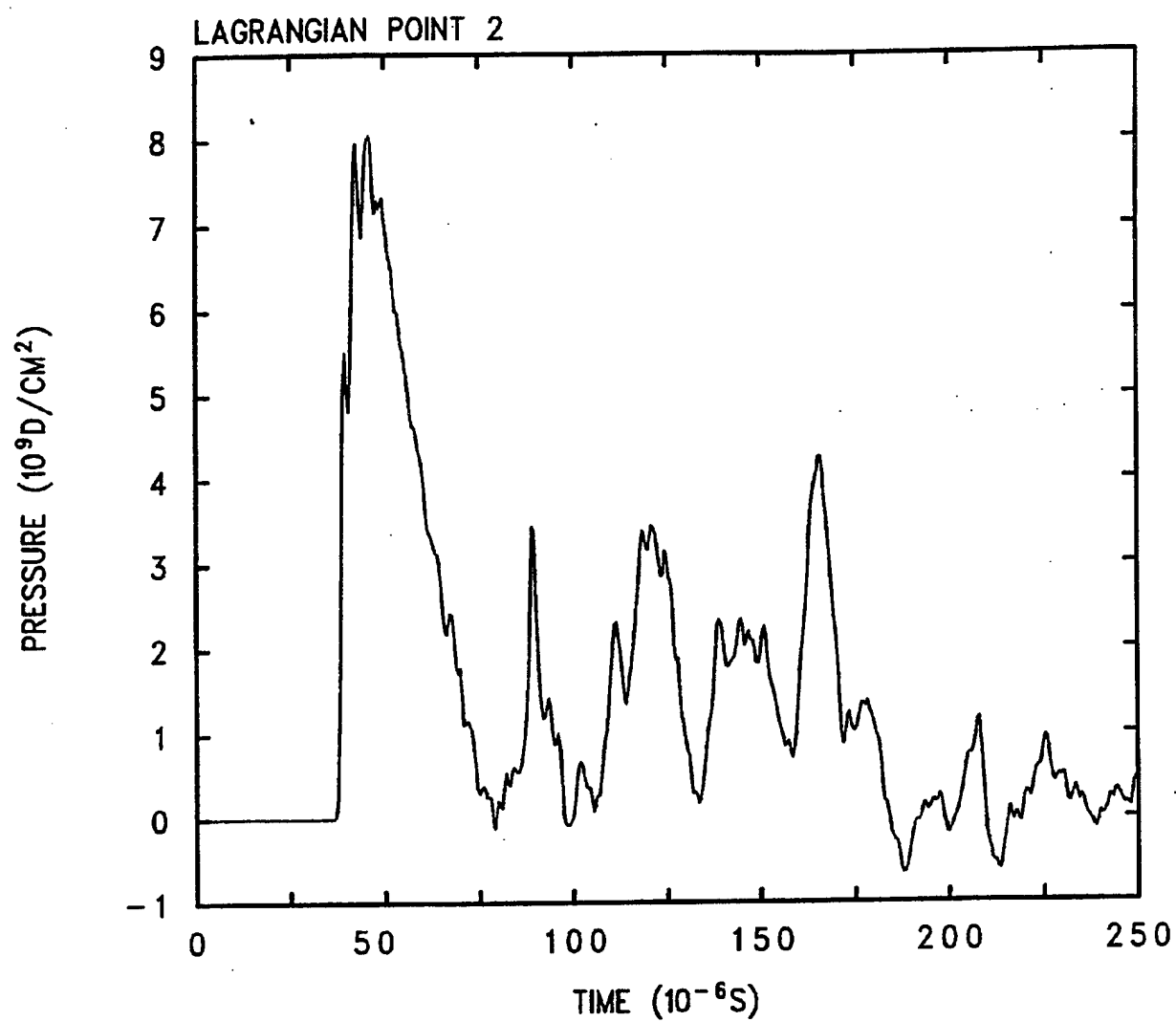


Figure 4. 76-mm Plexiglas buffer: pressure history.

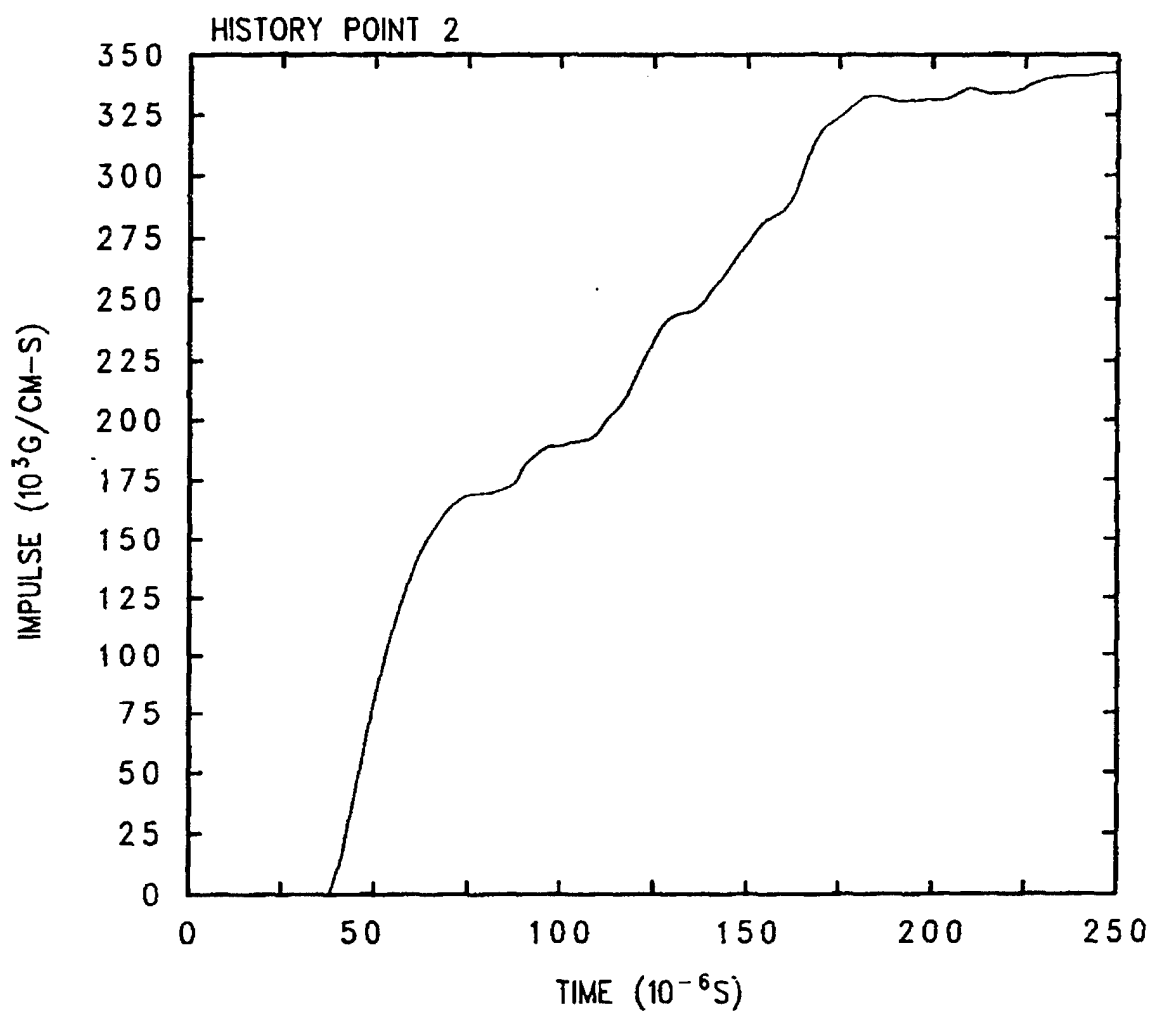


Figure 5. 76-mm Plexiglas buffer: impulse history.

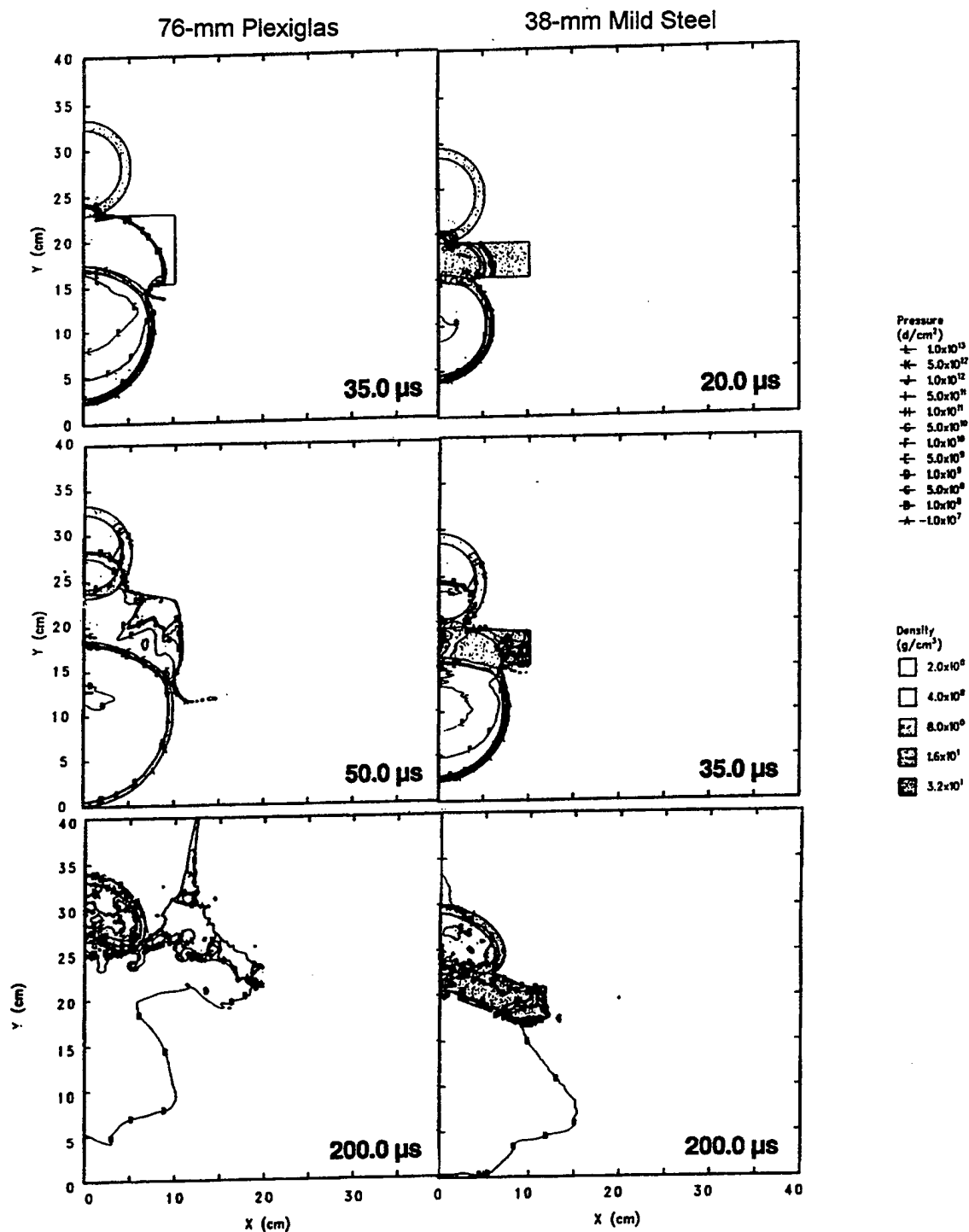


Figure 6. Plexiglas and mild steel: comparison of pressure contours.

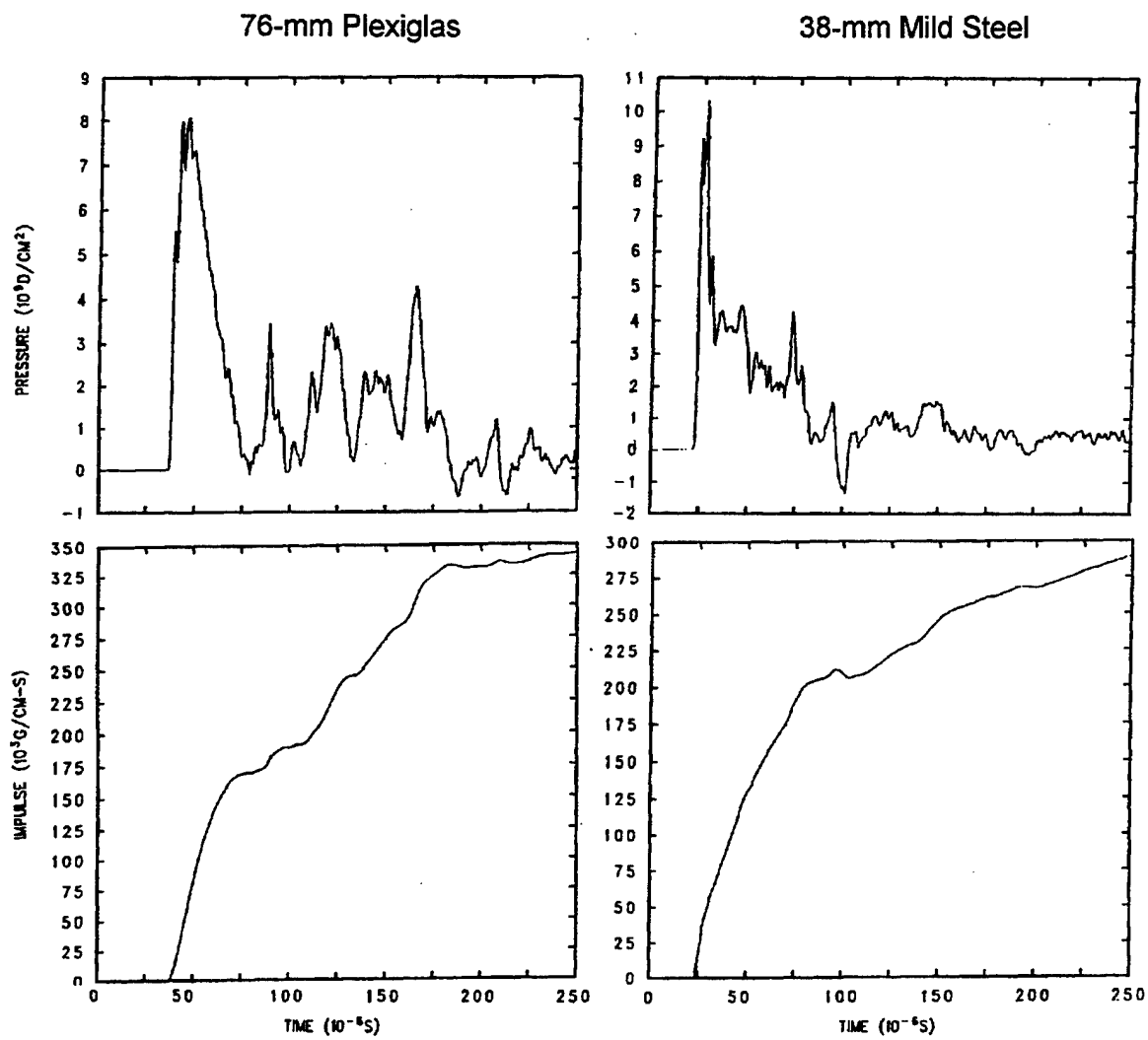


Figure 7. Plexiglas and mild steel: comparison of pressure and impulse histories.



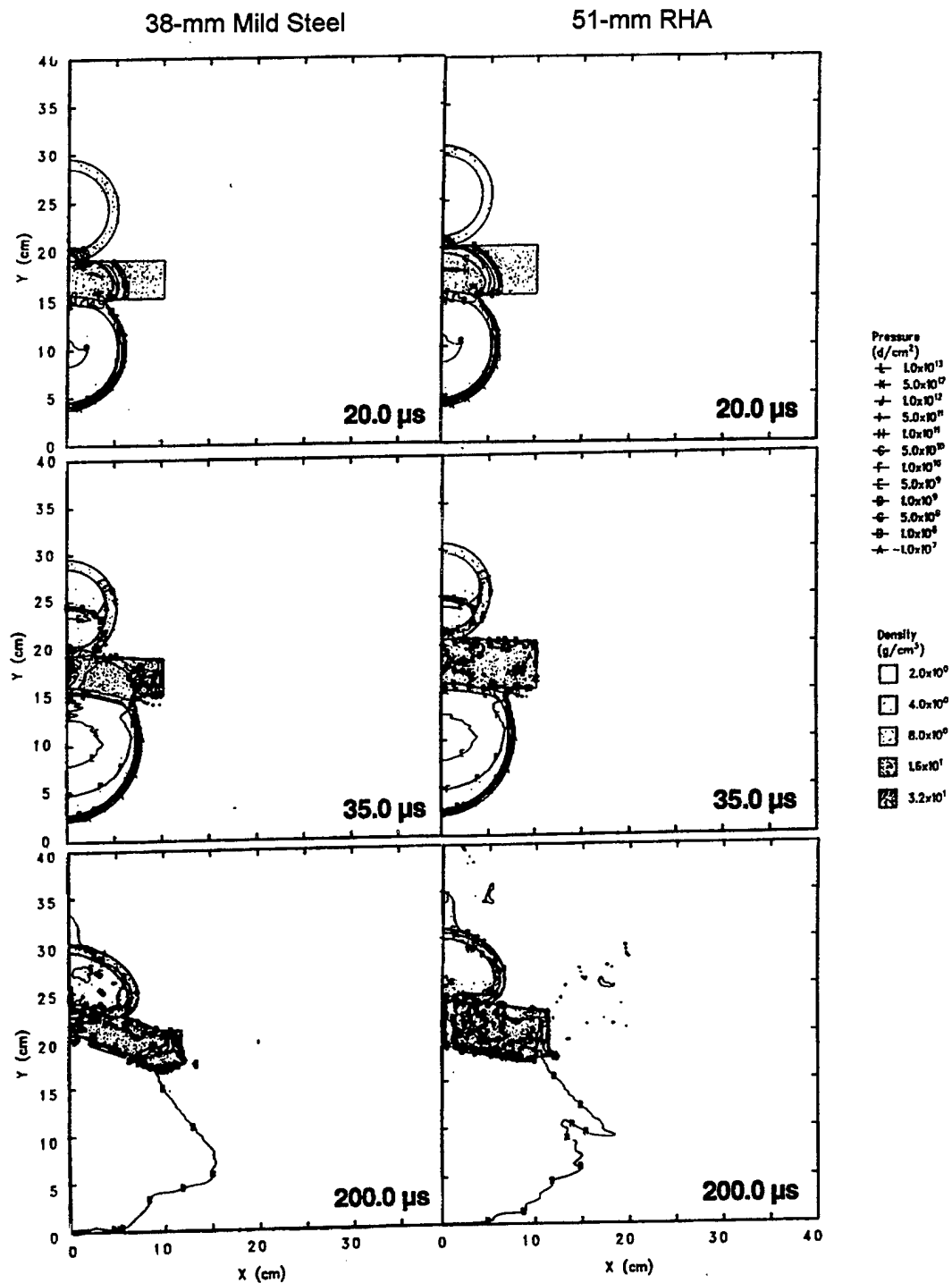


Figure 8. Mild steel and RHA: comparison of pressure contours at the experimental threshold.

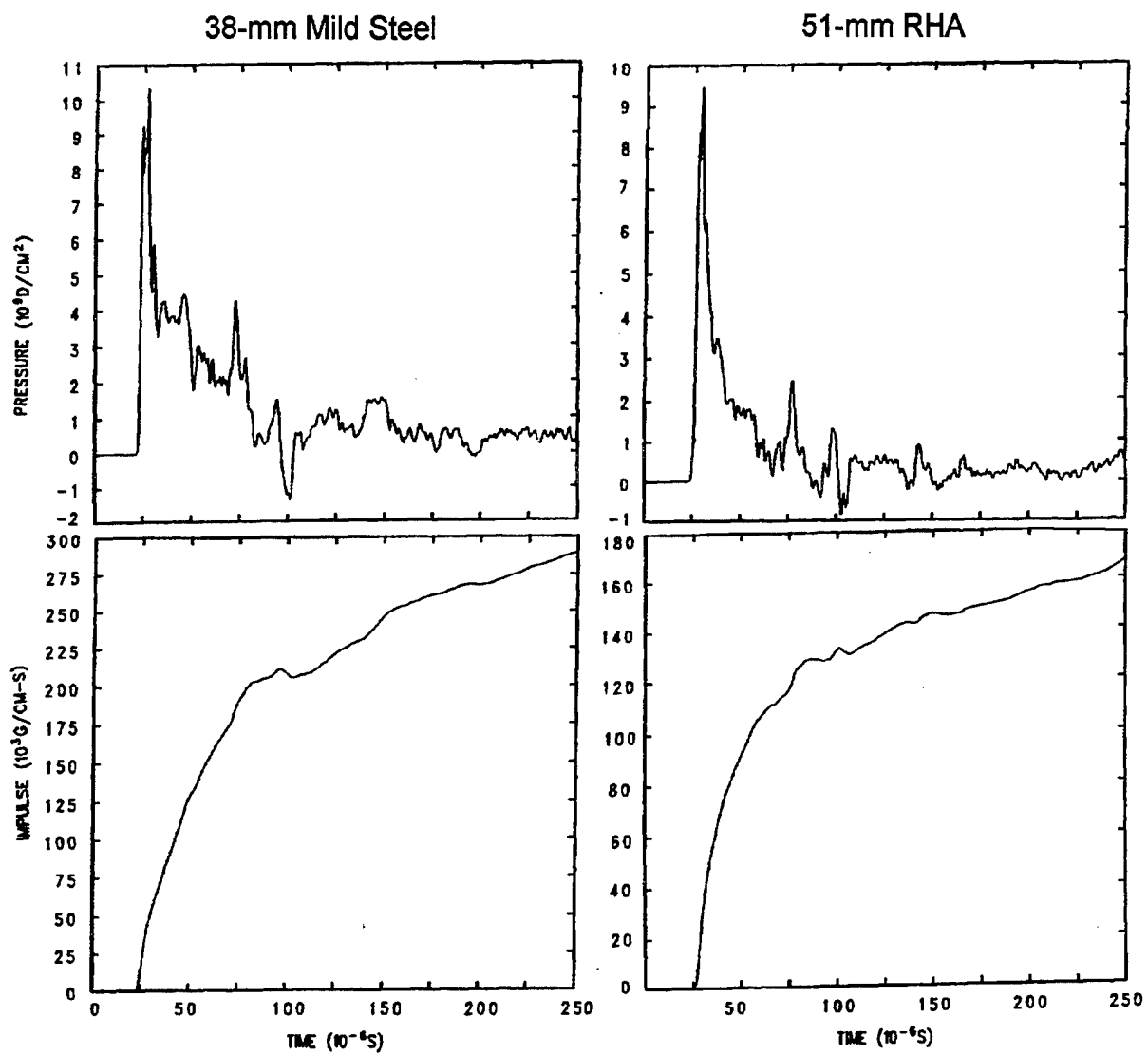


Figure 9. Mild steel and RHA: comparison of pressure and impulse histories at the experimental threshold.

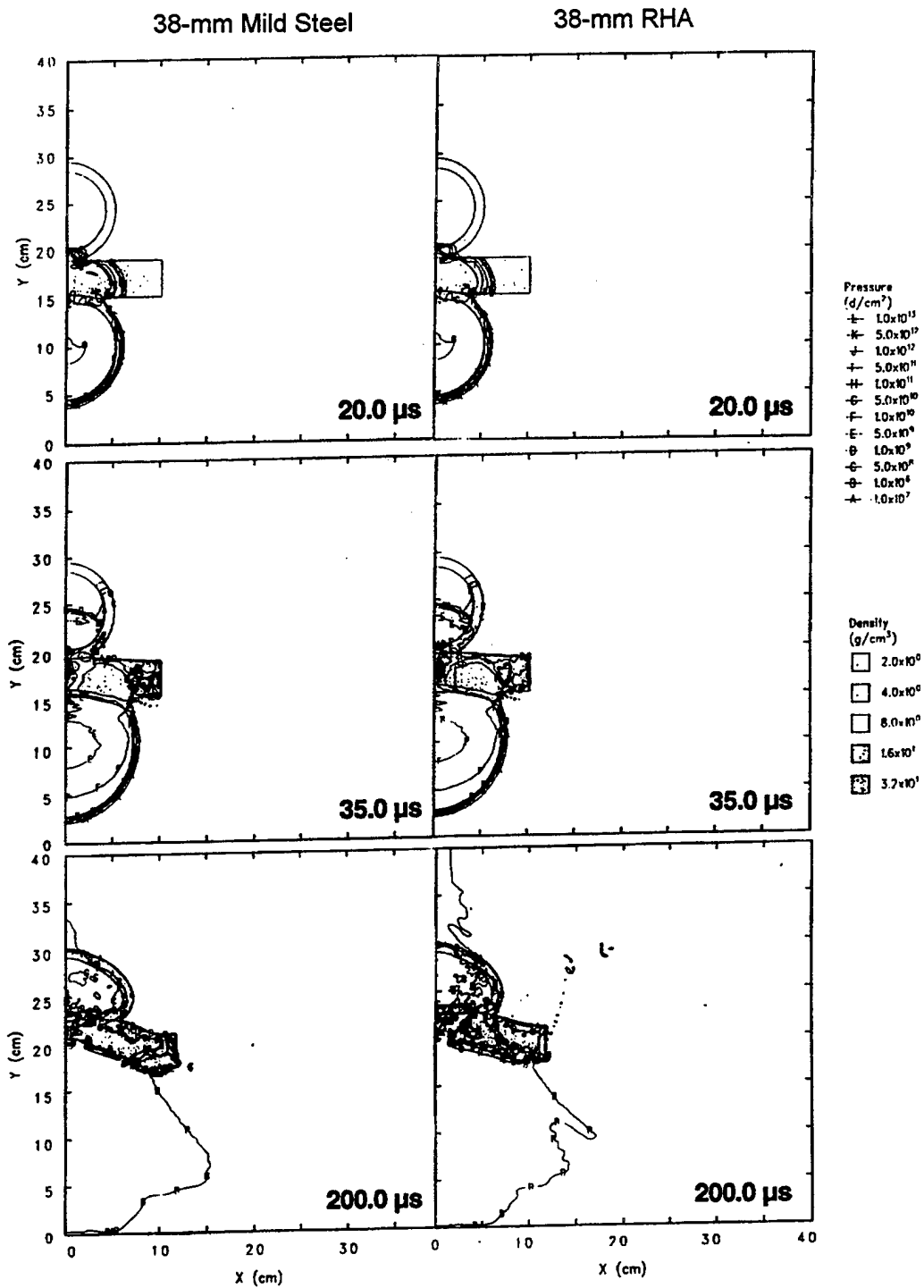


Figure 10. Mild steel and RHA: comparison of pressure contours at the same buffer thickness.

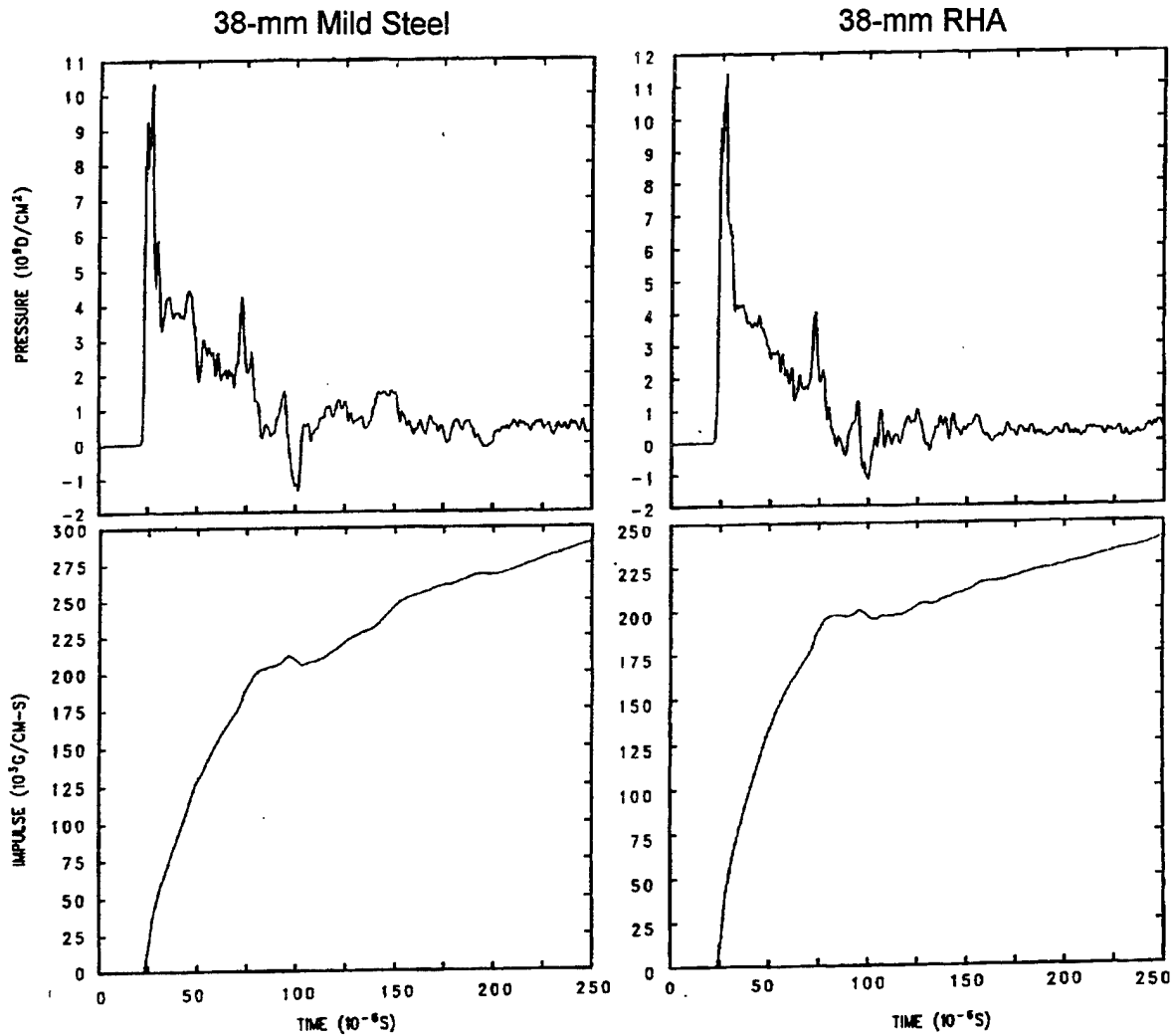


Figure 11. Mild steel and RHA: comparison of pressure and impulse histories at the same buffer thickness.

Table 2. Computed Pressure and Impulse at the Experimental Thresholds

BUFFER MATERIAL	BUFFER THICKNESS (mm)	PEAK PRESSURE (GPa)	FIRST-PULSE IMPULSE (kPa•s)	ULTIMATE IMPULSE (kPa•s)
PLEXIGLAS	70	0.94	17.6	36.0
	76	0.81	16.9	34.2
MILD STEEL	32	1.22	24.7	35.1
	38	1.28	20.3	28.8
RHA	51	0.94	12.9	16.8

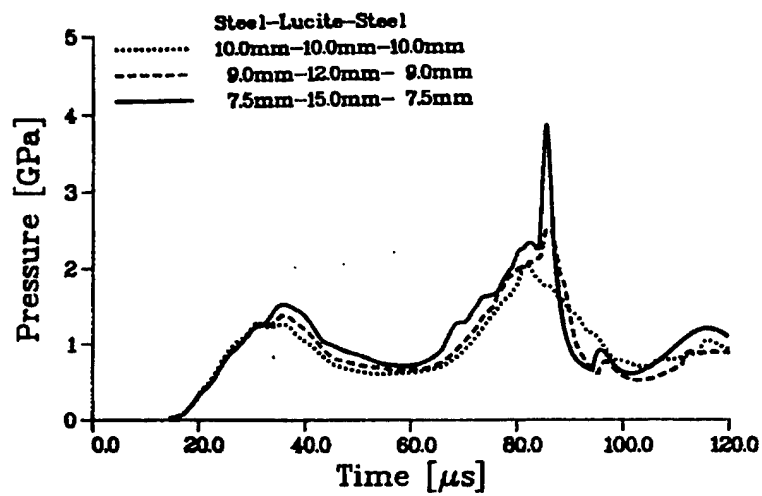
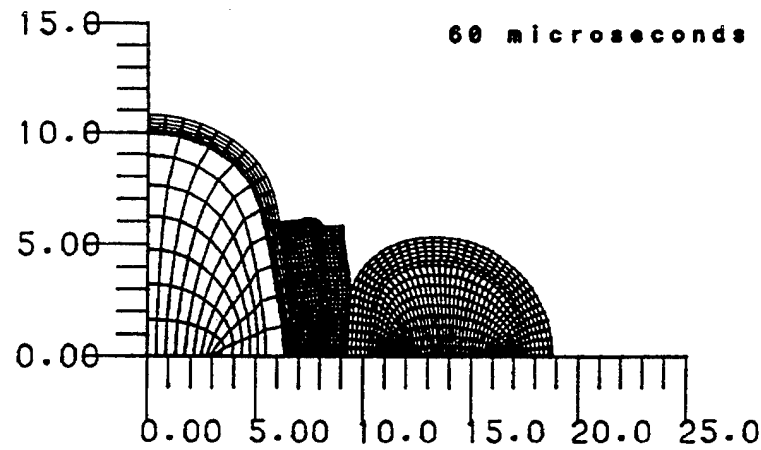


Figure 12. Results of the STEALTH sympathetic detonation simulation with layered buffers.

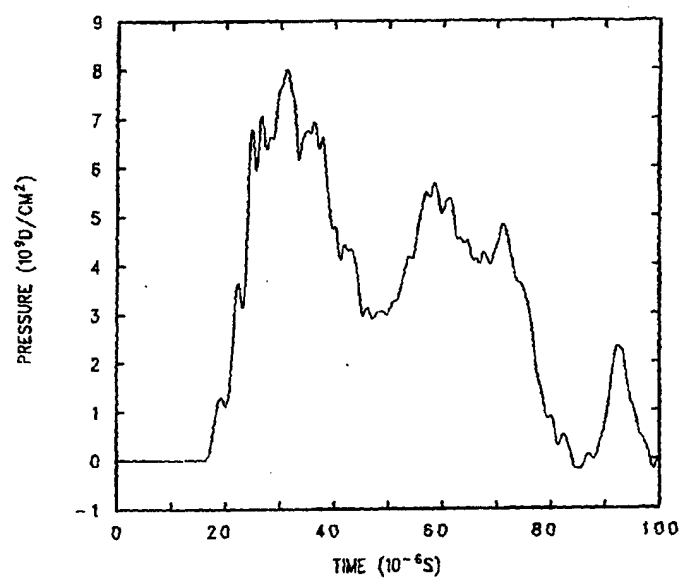
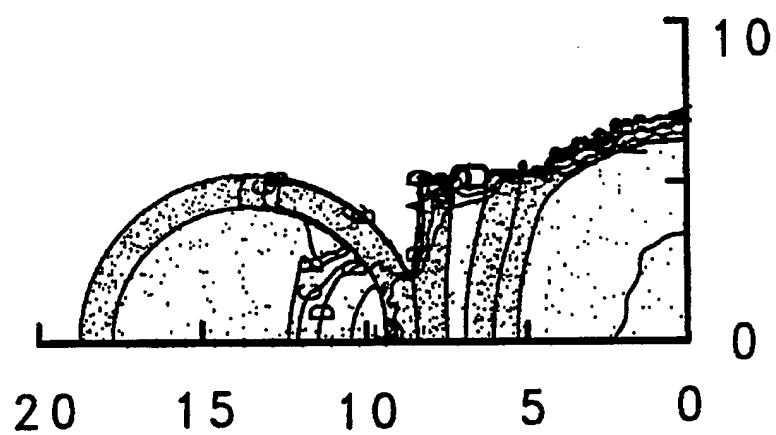


Figure 13. Results of the CTH sympathetic detonation simulation with layered buffers.

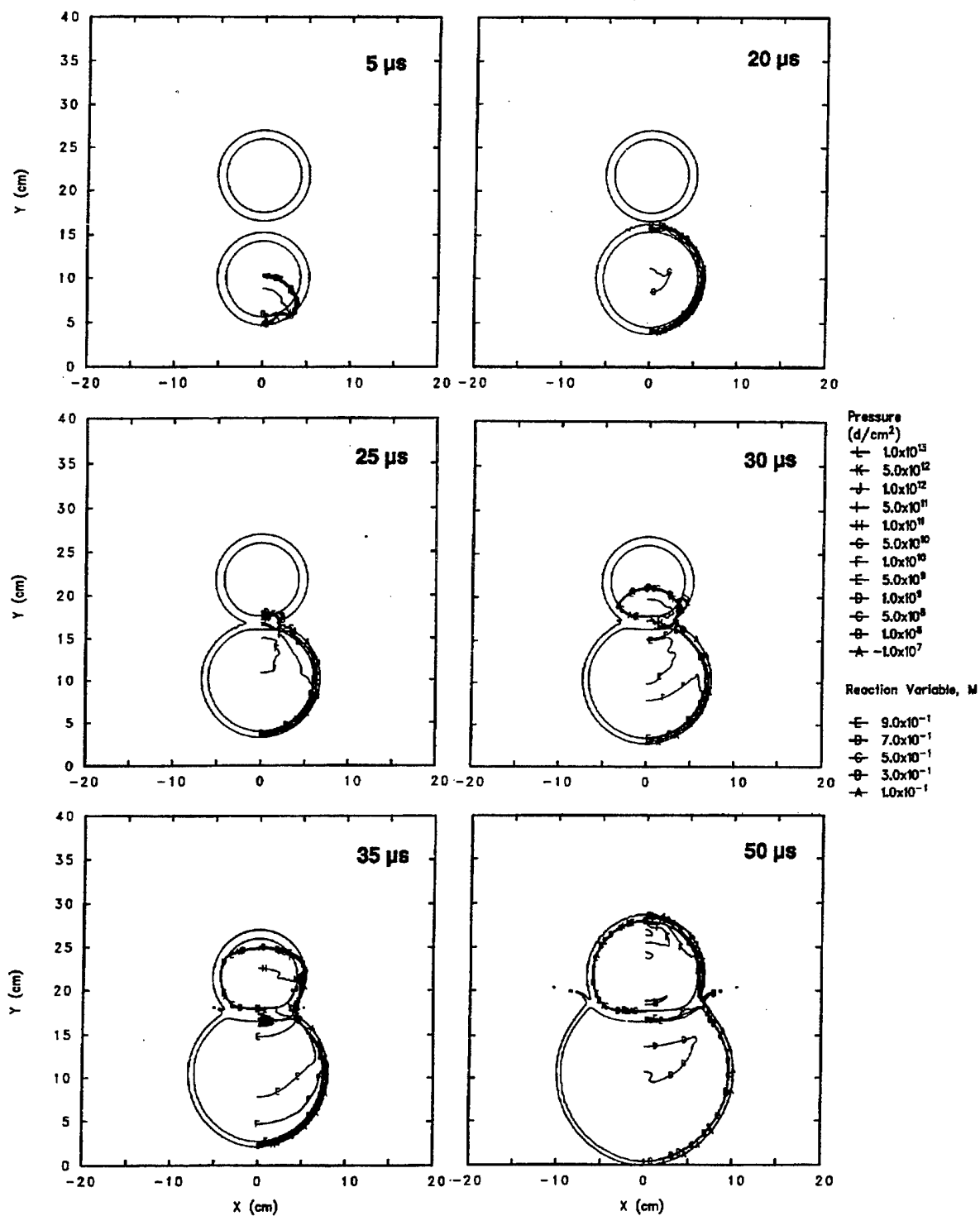


Figure 14. Unbuffered configuration with 12.7-mm separation: pressure and reaction variable contours.



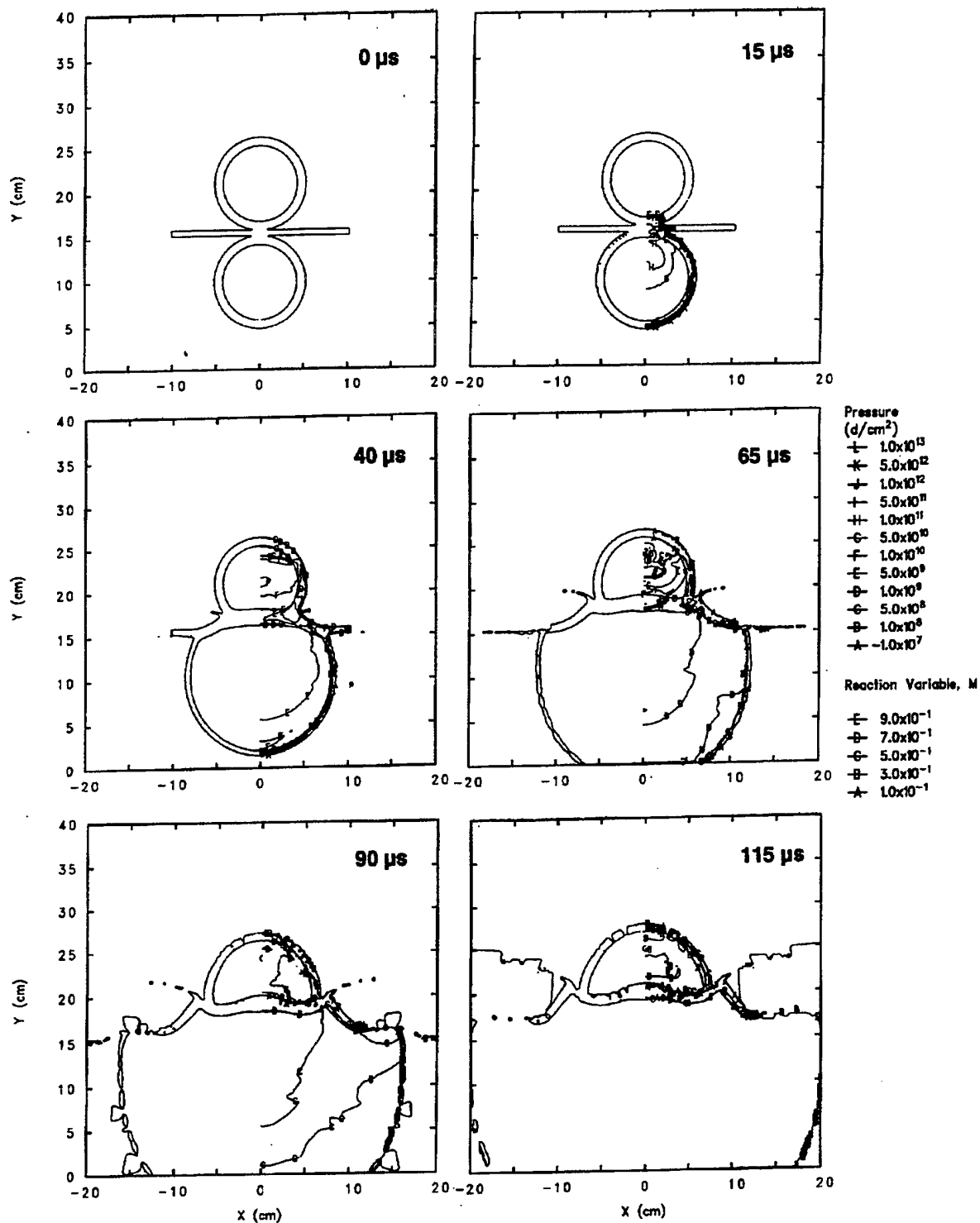


Figure 15. 6.4-mm Steel buffer in direct contact with donor and acceptor munitions: pressure and reaction variable contours.

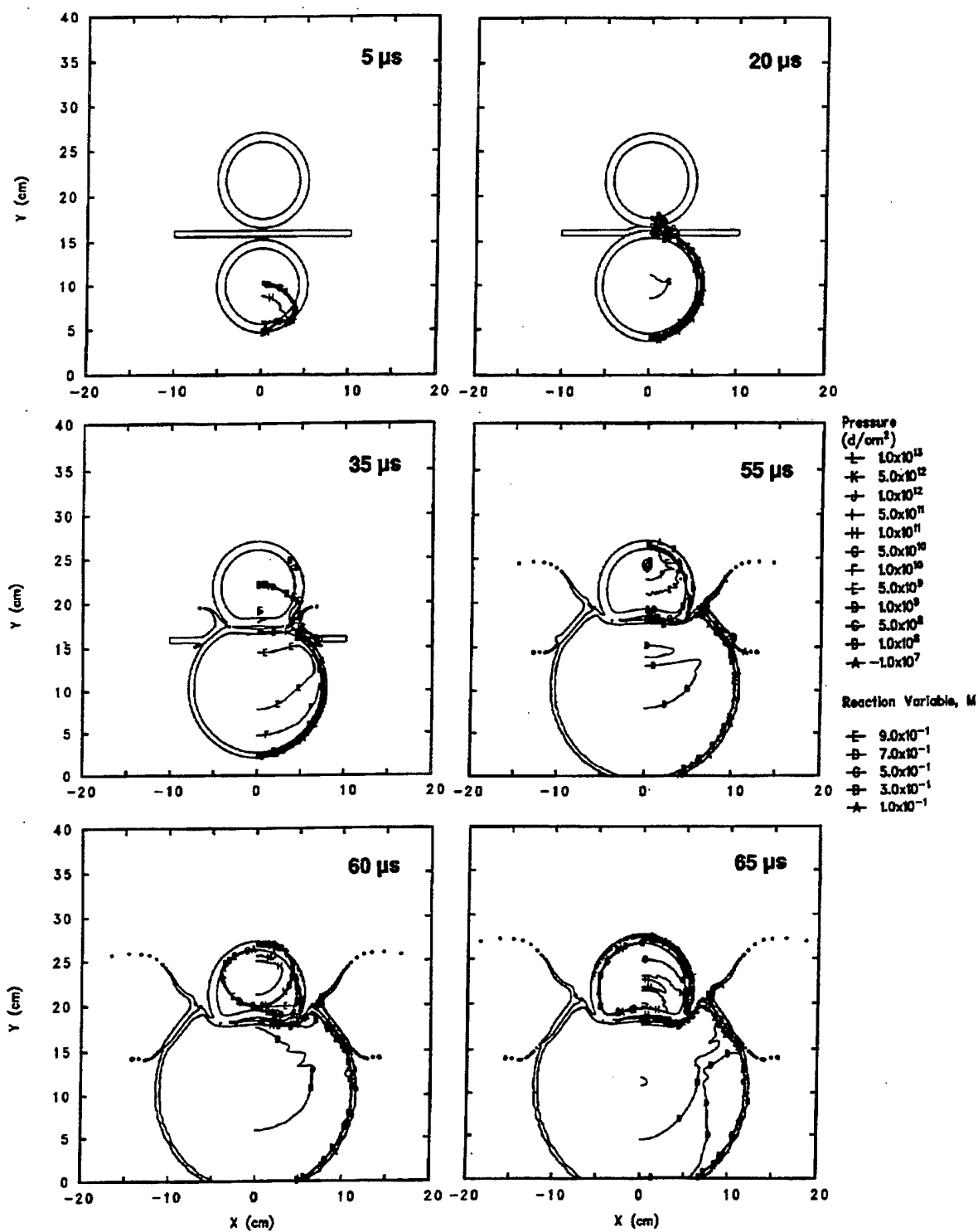


Figure 16. 6.4-mm Plexiglas buffer centered in 12.7-mm space: pressure and reaction variable contours.

Table 3. Sympathetic Detonation Predictions for the Contact Configurations

BUFFER THICKNESS (mm)	STEEL	PLEXIGLAS	AIR
3.2	GO (reflected wave, ~45 $\mu$ s)	GO (reflected wave, ~50 $\mu$ s)	
6.4	NOGO	NOGO	GO (incident wave, ~23 $\mu$ s)
12.7		NOGO	GO (incident wave, ~27 $\mu$ s)

Table 4. HVRB Results for 12.7-mm Munition-to-munition Separation Computations.

BUFFER THICKNESS (mm)	STEEL	PLEXIGLAS	AIR
1.6	GO (incident wave, ~30 $\mu$ s)	GO (incident wave, ~25 $\mu$ s)	
3.2	NOGO	GO (incident wave, ~25 $\mu$ s)	
6.4	NOGO	GO (reflected wave, ~55 $\mu$ s)	
12.7			GO (incident wave, ~27 $\mu$ s)

## 8. REFERENCES

- Boyle, V. Personal Communication. U.S. Army Research Laboratory, Aberdeen Proving Ground, MD, 1995.
- Electric Power Research Institute. "STEALTH - A Lagrange Explicit Finite Difference Code for Solids, Structural, and Thermohydraulic Analysis." Palo Alto, CA. November 1981.
- Hertel, E. S. , Jr., R. L. Bell, M. G. Elrick, A. V. Farnsworth, G. I. Kerley, J. M. McGlaun, S. V. Petney, S. A. Silling, P. A. Taylor, and L. Yarrington. "CTH: A Software Family for Multi-Dimensional Shock Physics Analysis." Proceedings of the 19th International Symposium on Shock Waves, Vol. 1, pp 377-382, July 1993.
- Kerley, G. I. "CTH Equation of State Package: Porosity and Reactive Burn Models." Sandia Report SAND92-0553, April 1992.
- Starkenber, J., Y. K. Huang, and A. L. Arbuckle. "A Two-Dimensional Numerical Study of Detonation Propagation Between Munitions by Means of Shock Initiation." BRL-TR-02522, U.S. Army Ballistic Research Laboratory, Aberdeen Proving Ground, MD, September, 1983.
- Starkenber, J., T. M. Dorsey, K. J. Benjamin, A. L. Arbuckle. "A Computational Investigation of Shielding Effectiveness in Mitigating Stimuli Associated With the Sympathetic Detonation of Munitions." BRL-TR-2879, U.S. Army Ballistic Research Laboratory, Aberdeen Proving Ground, MD. December 1987.

INTENTIONALLY LEFT BLANK.

NO. OF  
COPIES ORGANIZATION

2 DEFENSE TECHNICAL  
INFORMATION CENTER  
DTIC DDA  
8725 JOHN J KINGMAN RD  
STE 0944  
FT BELVOIR VA 22060-6218

1 HQDA  
DAMO FDQ  
DENNIS SCHMIDT  
400 ARMY PENTAGON  
WASHINGTON DC 20310-0460

1 CECOM  
SP & TRRSTRL COMMCTN DIV  
AMSEL RD ST MC M  
H SOICHER  
FT MONMOUTH NJ 07703-5203

1 PRIN DPTY FOR TCHNLGY HQ  
US ARMY MATCOM  
AMCDCG T  
M FISETTE  
5001 EISENHOWER AVE  
ALEXANDRIA VA 22333-0001

1 PRIN DPTY FOR ACQUSTN HQS  
US ARMY MATCOM  
AMCDCG A  
D ADAMS  
5001 EISENHOWER AVE  
ALEXANDRIA VA 22333-0001

1 DPTY CG FOR RDE HQS  
US ARMY MATCOM  
AMCRD  
BG BEAUCHAMP  
5001 EISENHOWER AVE  
ALEXANDRIA VA 22333-0001

1 ASST DPTY CG FOR RDE HQS  
US ARMY MATCOM  
AMCRD  
COL S MANESS  
5001 EISENHOWER AVE  
ALEXANDRIA VA 22333-0001

NO. OF  
COPIES ORGANIZATION

1 DPTY ASSIST SCY FOR R&T  
SARD TT F MILTON  
THE PENTAGON RM 3E479  
WASHINGTON DC 20310-0103

1 DPTY ASSIST SCY FOR R&T  
SARD TT D CHAIT  
THE PENTAGON  
WASHINGTON DC 20310-0103

1 DPTY ASSIST SCY FOR R&T  
SARD TT K KOMINOS  
THE PENTAGON  
WASHINGTON DC 20310-0103

1 DPTY ASSIST SCY FOR R&T  
SARD TT B REISMAN  
THE PENTAGON  
WASHINGTON DC 20310-0103

1 DPTY ASSIST SCY FOR R&T  
SARD TT T KILLION  
THE PENTAGON  
WASHINGTON DC 20310-0103

1 OSD  
OUSD(A&T)/ODDDR&E(R)  
J LUPO  
THE PENTAGON  
WASHINGTON DC 20301-7100

1 INST FOR ADVNCD TCHNLGY  
THE UNIV OF TEXAS AT AUSTIN  
PO BOX 202797  
AUSTIN TX 78720-2797

1 DUSD SPACE  
1E765 J G MCNEFF  
3900 DEFENSE PENTAGON  
WASHINGTON DC 20301-3900

1 USAASA  
MOAS AI W PARRON  
9325 GUNSTON RD STE N319  
FT BELVOIR VA 22060-5582

NO. OF  
COPIES ORGANIZATION

1 CECOM  
PM GPS COL S YOUNG  
FT MONMOUTH NJ 07703

1 GPS JOINT PROG OFC DIR  
COL J CLAY  
2435 VELA WAY STE 1613  
LOS ANGELES AFB CA 90245-5500

1 ELECTRONIC SYS DIV DIR  
CECOM RDEC  
J NIEMELA  
FT MONMOUTH NJ 07703

3 DARPA  
L STOTTS  
J PENNELLA  
B KASPAR  
3701 N FAIRFAX DR  
ARLINGTON VA 22203-1714

1 SPCL ASST TO WING CMNDR  
50SW/CCX  
CAPT P H BERNSTEIN  
300 O'MALLEY AVE STE 20  
FALCON AFB CO 80912-3020

1 USAF SMC/CED  
DMA/JPO  
M ISON  
2435 VELA WAY STE 1613  
LOS ANGELES AFB CA 90245-5500

1 US MILITARY ACADEMY  
MATH SCI CTR OF EXCELLENCE  
DEPT OF MATHEMATICAL SCI  
MDN A MAJ DON ENGEN  
THAYER HALL  
WEST POINT NY 10996-1786

1 DIRECTOR  
US ARMY RESEARCH LAB  
AMSRL CS AL TP  
2800 POWDER MILL RD  
ADELPHI MD 20783-1145

NO. OF  
COPIES ORGANIZATION

1 DIRECTOR  
US ARMY RESEARCH LAB  
AMSRL CS AL TA  
2800 POWDER MILL RD  
ADELPHI MD 20783-1145

3 DIRECTOR  
US ARMY RESEARCH LAB  
AMSRL CI LL  
2800 POWDER MILL RD  
ADELPHI MD 20783-1145

ABERDEEN PROVING GROUND

2 DIR USARL  
AMSRL CI LP (305)



<u>NO. OF COPIES</u>	<u>ORGANIZATION</u>
1	DIR LANL ATTN PHILIP M HOWE PO BOX 1663 LOS ALAMOS NM 87545
1	DIR LANL ATTN WILLIAM C DAVIS 693 46TH STREET LOS ALAMOS NM 87545
1	DIR LLNL ATTN CRAIG M TARVER PO BOX 808 LIVERMORE CA 94550
1	DIR SANDIA NATIONAL LAB ATTN EUGENE S HERTEL PO BOX 5800 ALBUQUERQUE NM 87185-5800
3	CDR NVL SURFC WARFARE CTR ATTN RICHARD R BERNECKER KIBONG KIM HAROLD W SANDUSKY 10901 NEW HAMPSHIRE AVE SILVER SPRING MD 20903-5640
1	CDR NVL SURFC WARFARE CTR INDIAN HEAD DIV ATTN RUTH M DOHERTY CODE 9230D 101 STRAUSS AVE INDIAN HEAD MD 20640-5035
1	CDR US ARMY ARDEC ATTN BARRY D FISHBURN VLADIMIR M GOLD PICATINNY ARSENAL NJ 07806-5000
1	KERLEY PUBLISHING SERVICES ATTN GERALD I KERLEY PO BOX 13835 ALBUQUERQUE NM 87192-3835
1	DYNA EAST CORP ATTN PEI CHI CHOU 3201 ARCH STREET PHILADELPHIA PA 19104

<u>NO. OF COPIES</u>	<u>ORGANIZATION</u>
1	VANDERBILT UNIV ATTN ARTHUR M MELLOR BOX 1592 NASHVILLE TN 37235-1592
1	GRYTING ENERGETICS SCIENCE CO ATTN HAROLD J GRYTING 7126 SHADOW RUN SAN ANTONIO TX 78250-3483
1	DIR WRIGHT LAB ARMAMENT DIRECTORATE ATTN J GREGORY GLENN EGLIN AIR FORCE BASE FL 32542-5434
	<u>ABERDEEN PROVING GROUND</u>
8	DIR USARL ATTN AMSRL WM T, W MORRISON AMSRL WM TB, R FREY J WATSON V BOYLE W LAWRENCE S SCHRAML E MCDOUGAL T DORSEY

NO. OF  
COPIES ORGANIZATION

- 2 AGENCY FOR DEFENSE DEV  
ATTN JAIMIN LEE  
SO YONG SONG  
YUSEONG PO BOX 35 (1-3-7)  
TAEJON 305-600 KOREA
- 2 FRENCH GERMAN RSRCH INST (ISL)  
ATTN HENRY P A MOULARD  
MICHEL M S SAMIRANT  
5 RUE DE GENERAL CASSAGNOU  
SAINT LOUIS CEDEX 68301 FRANCE
- 1 DEFENCE RSRCH ESTAB VALCARTIER  
ATTN CONRAD BELANGER  
2459 PIE XI BOULEVARD NORTH  
QUEBEC GOA 1R0 CANADA
- 1 DEFENCE RESEARCH AGENCY  
ATTN PETER J HASKINS  
FORT HALSTEAD  
SEVENOAKS KENT TN14 7BP  
ENGLAND

REPORT DOCUMENTATION PAGE			Form Approved OMB No. 0704-0188	
<small>Public reporting burden for this collection of information is estimated to average 1 hour per response, including the time for reviewing instructions, searching existing data sources, gathering and maintaining the data needed, and completing and reviewing the collection of information. Send comments regarding this burden estimate or any other aspect of this collection of information, including suggestions for reducing this burden, to Washington Headquarters Services, Directorate for Information Operations and Reports, 1215 Jefferson Davis Highway, Suite 1204, Arlington, VA 22202-4302, and to the Office of Management and Budget, Paperwork Reduction Project(0704-0188), Washington, DC 20503.</small>				
1. AGENCY USE ONLY (Leave blank)	2. REPORT DATE June 1997	3. REPORT TYPE AND DATES COVERED Final, Oct 94-Sep 96		
4. TITLE AND SUBTITLE  Simulating Sympathetic Detonation of 105-mm Artillery Projectiles With CTH		5. FUNDING NUMBERS  PR: 1L162618AH80		
6. AUTHOR(S)  Kelly J. Benjamin and John Starkenberg				
7. PERFORMING ORGANIZATION NAME(S) AND ADDRESS(ES)  U.S. Army Research Laboratory ATTN: AMSRL-WM-TB Aberdeen Proving Ground, MD 21005-5066		8. PERFORMING ORGANIZATION REPORT NUMBER  ARL-TR-1365		
9. SPONSORING/MONITORING AGENCY NAMES(S) AND ADDRESS(ES)		10. SPONSORING/MONITORING AGENCY REPORT NUMBER		
11. SUPPLEMENTARY NOTES				
12a. DISTRIBUTION/AVAILABILITY STATEMENT  Approved for public release; distribution is unlimited.		12b. DISTRIBUTION CODE		
13. ABSTRACT (Maximum 200 words) <p>The CTH code was used to simulate sympathetic detonation experiments conducted using 105-mm projectiles separated by buffers of Plexiglas, rolled homogeneous armor (RHA), and mild steel. Buffer thicknesses near the experimental sympathetic detonation threshold were simulated. No propagation criterion associated with pressure loading was revealed by the results of this study. CTH computations were also made to confirm the presence of finite rise-time or "ramp" waves in the acceptor explosive (previously observed in Lagrangian computations) with layered buffers of Plexiglas and steel. The CTH results show more structure in the ramp wave and shorter rise times than those previously obtained. The History Variable Reactive Burn (HVRB) explosive initiation model in the CTH code was exercised in simulations of similar configurations. These simulations showed that initiation may occur during propagation of the incident shock wave through the acceptor or after its reflection from the casing at the back of the acceptor. Predicted buffer thicknesses required to prevent sympathetic detonation are much less than those determined in the experiments, indicating that mechanisms in addition to shock initiation contribute to sympathetic detonation.</p>				
14. SUBJECT TERMS  explosives, munitions, sympathetic detonation		15. NUMBER OF PAGES 35		
		16. PRICE CODE		
17. SECURITY CLASSIFICATION OF REPORT UNCLASSIFIED	18. SECURITY CLASSIFICATION OF THIS PAGE UNCLASSIFIED	19. SECURITY CLASSIFICATION OF ABSTRACT UNCLASSIFIED	20. LIMITATION OF ABSTRACT  UL	

INTENTIONALLY LEFT BLANK.

## USER EVALUATION SHEET/CHANGE OF ADDRESS

This Laboratory undertakes a continuing effort to improve the quality of the reports it publishes. Your comments/answers to the items/questions below will aid us in our efforts.

1. ARL Report Number/Author ARL-TR-1365 (Benjamin) Date of Report June 1997

2. Date Report Received \_\_\_\_\_

3. Does this report satisfy a need? (Comment on purpose, related project, or other area of interest for which the report will be used.) \_\_\_\_\_  
\_\_\_\_\_  
\_\_\_\_\_

4. Specifically, how is the report being used? (Information source, design data, procedure, source of ideas, etc.) \_\_\_\_\_  
\_\_\_\_\_  
\_\_\_\_\_

5. Has the information in this report led to any quantitative savings as far as man-hours or dollars saved, operating costs avoided, or efficiencies achieved, etc? If so, please elaborate. \_\_\_\_\_  
\_\_\_\_\_  
\_\_\_\_\_

6. General Comments. What do you think should be changed to improve future reports? (Indicate changes to organization, technical content, format, etc.) \_\_\_\_\_  
\_\_\_\_\_  
\_\_\_\_\_  
\_\_\_\_\_

CURRENT  
ADDRESS

\_\_\_\_\_  
Organization

\_\_\_\_\_  
Name

\_\_\_\_\_  
E-mail Name

\_\_\_\_\_  
Street or P.O. Box No.

\_\_\_\_\_  
City, State, Zip Code

7. If indicating a Change of Address or Address Correction, please provide the Current or Correct address above and the Old or Incorrect address below.

OLD  
ADDRESS

\_\_\_\_\_  
Organization

\_\_\_\_\_  
Name

\_\_\_\_\_  
Street or P.O. Box No.

\_\_\_\_\_  
City, State, Zip Code

(Remove this sheet, fold as indicated, tape closed, and mail.)  
(DO NOT STAPLE)